GLOBAL Scientific Inc. CHEMXPRESS

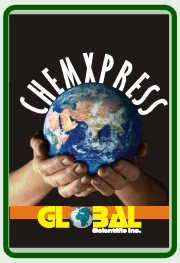

ORIGINAL ARTICLE

New phosphorous hardeners intercalated epoxy/clay nanocomposites enhanced in homogeneity, modulus and heat resistant properties

M.Suguna Lakshmi*, B.S.R.Reddy
Industrial Chemistry Laboratory, Central Leather Research Institute, Chennai, 600 020, (INDIA)
E-mail: lakshmi.suguna@gmail.com
Received: 9th November, 2012 ; Accepted: 7th February, 2013

Abstract: Different phosphorous hardeners (PHs) 4,4'-diaminodiphenylether (DDE), 4,4'-diaminodiphenylmethane (DDM) and 4,4'-diaminodiphenylsulphone (DDS) were successfully synthesized These PHs could be used as a better choice of curatives because of their inherent thermal resistance and better organic solubility characteristics. Using the PHs, a series of unmodified epoxy (UME) composites and clay modified epoxy (CME) nanocomposites were prepared. The UME composites were stable up to 468ºC. The limiting oxygen index (LOI) of CME was higher than that of UME. This was due to the flame retardancy obtained through the synergistic effect of phosphorous and nanoclay in the CME nanocomposites.

Keywords: Resins; Cure; Thermomechanical; Thermal properties.

ORIGINAL ARTICLE

INTRODUCTION

The area of polymer/clay nanocomposites has received widespread interest in the past two decades. Much effort has been centered on the development of epoxy/clay nanocomposites using normal and organomodified clay minerals[1–4]. Epoxy–clay nanocomposite is one of the most potential materials that have offered the prospects of emerging new hybrid material with desired characteristics using the clay minerals for numerous applications[5–7]. Chemical modification of epoxy matrix is a key step in making nanocomposites for advanced material applications. One of the main drawbacks hindering these applications is the low thermal stability of epoxy molecules. This makes these materials unserviceable at higher temperatures[8–11]. The incorporation of phosphorous molecules as a part of the backbone in engineering plastics have showed increased flame retardation, high char formation and low rates of heat release property[12]. In this paper, we have adopted a unique approach towards increasing flame retardance and toughness of epoxy materials by employing newly synthesised PHs. The PHs having amino group at one end, aids the crosslink network formation and the ethyl groups available at the other end is capable of compatibilizing the hydrophobic segments like polydimethylsiloxane polymers into DGEBA-epoxy resins. Thus the enhanced toughness, thermal stability and bonding strength property of the materials have been reported by us[13].

The major objective of the present study is to investigate the effect of PHs primarily on thermal and mechanical properties in UME and CME materials. Here, we have reported the synthesis and characterization of the PHs prepared using diethylchlorophosphate and three diamines (DDE, DDM and DDS). Series of CME nanocomposites were then prepared by blending with the clay. The chemical functionalization of P-hardener with epoxy resins and montmorillonite was carried out to improve heat resistance property, viscoelastic behavior and flame retardancy of the CME materials. We have exclusively studied the thermomechanical and thermal degradation kinetic mechanisms of UME and CME materials.

EXPERIMENTAL

Materials

Diethylchlorophosphate, diaminodiphenylsulphone, diaminodiphenylmethane, diaminodiphenylether, triethylamine and NANOMER1.30E (MMT clay surface modified with octadecyl amine, a primary amine base) was obtained from Aldrich and used as received. Tetrahydrofuran and ethyl acetate were supplied by SD fine chem. India. Diglycidylether of bisphenol A resin (DGEBA, LY556, EEW 180-185, density 1.23, refractive index 1.57, and viscosity~10,000 CP) was supplied by Ciba specialty chemicals India.

Characterization

The FTIR spectra were obtained using a Nicolet (model 20DXB) spectrophotometer with KBr pellets for solid specimens within scanning range of 400-4000 cm^{-1}. The microstructure and the extent of dispersion of the nanoclay particles in the epoxy matrix were investigated using a wide angle X-ray diffraction (WXRD). The WXRD measurement of the samples was performed at the rate of 2°/min with Cu K_{α} radiation (λ=1.5401 A°) at a generator voltage of 40 kV and current of 100 mA. The thermogravimetric analyses (TGA) were performed using a TA Instruments Q50 under air atmosphere at a flow rate of 60 mL/min. The samples were heated from 40° to 800°C at a heating rate of 20°C/min. The storage modulus and glass transition temperature (Tg) of the nanocomposites were measured with dynamic mechanical analysis (Netzsch proteus) in a 3-point bending mode. The analyses were performed at a frequency of 1 Hz and a temperature range of 40 - 250°C at a heating rate of 3°C/min.

Synthesis of P-hardeners

Diethylchlorophosphate (34.51g, 0.2mole) dissolved in tetrahydrofuran (50 ml) was charged into a ice cooled 250ml-3-neck round bottom flask equipped with a magnetic stirrer, thermometer and a nitrogen inlet. To this, 49.6g (0.210mole) of diaminodiphenyl-sulphone dissolved in 40ml THF was added drop wise and stirred. A 37.44g (0.217mole) of triethylamine was then added slowly and stirred

ORIGINAL ARTICLE

continuously for 3h. The triethylammonium bromide salt as a byproduct was settled to the bottom of the flask. The liquid phase containing the product was collected by filtration. The formation of diaminodiphenylsulphono-diethylphosphate (DDSDP) product was confirmed by FTIR and ^{1}H spectral analysis. Yield: 85%; Mol.wt:384. Similarly, diaminodiphenylmethane-diethylphosphate (DDMDP) (Yield: 88%; Mol.wt: 335), and diaminodiphenylether-diethylphosphate (DDEDP) (Yield: 79%; Mol.wt:337) was synthesized by reacting diethylcholorophosphate with diaminodiphenylmethane and diaminodiphenylether respectively.

Formulations of UME system

Blends of DGEBA and DDSDP or DDMDP or DDEDP were made employing the same equivalent ratios. The details of the blends were given in TABLE 1

TABLE 1 : The blends of DGEBA/P-hardener alone were denoted as UME (Unmodified Epoxy) systems and the blends of DGEBA/P-hardeners with clay were denoted as CME (Clay modified Epoxy) systems.

Sample Code	Epoxies	Curing agent	MMT (1.30E) clay
UME-DDSDP	DGEBA	DDSDP	-
UME-DDMDP	DGEBA	DDMDP	-
UME-DDEDP	DGEBA	DDEDP	-
CME-DDSDP	DGEBA	DDSDP	5%
CME-DDMDP	DGEBA	DDMDP	5%
CME-DDEDP	DGEBA	DDEDP	5%

The blends were thoroughly mixed at 120°C in an oil bath to get a homogeneous liquid. The reactants, were melted, homogenized and were transferred to a preheated open mold that was coated with silicon based sealant. Silicone based sealant was coated on the mold to ease releasing the samples from the mold after curing. The mold was preheated to 120°C before transferring the reaction mixture. After the material was transferred to the mold, it was heated to 130°C and deairated under vacuum for 0.5h to drive the air bubbles in the formulation. All the UME formulations were heated to 140°C and kept for 3h, 160°C for 2h and 180°C for 3h and cured. Then the cured laminates were removed from the mold and curing was continued at 180°C for 2h. The cured materials obtained were cut to suitable dimension required for characterization such as physical, chemical, thermal and mechanical properties.

Formulation of CME systems (Scheme 2)

Fifty parts of each epoxy and P-hardener were heated at 120°C. Then 5% clay was added to the resin bath and the mixing was carried out by mechanical shear mixer. The mixer rotates at 1000 rpm and the mixing was carried out for another 2h. After uniform mixing of clay and resin, respective hardener was added in to the resin- clay solution. All the formulations were prepared by using similar conditions adopted for preparing UME cured materials.

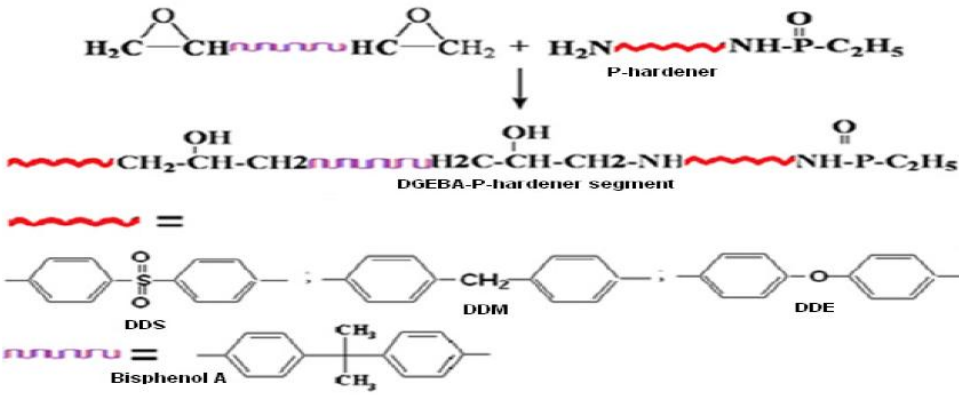

Scheme 1 : Reaction of DGEBA epoxy with P-hardeners.

RESULTS AND DISCUSSION

Spectroscopic analysis

The FTIR spectrum of all P–hardener was shown in Figure 1. The absorption bands of NH stretching vibration of primary amine groups (DDSDP, DDMDP and DDEDP) were observed at 3439, 3407 and 3269cm^{-1}, and NH bending vibrations at 1629, 1603 and 1675 cm^{-1} respectively. The characteristic band for

ORIGINAL ARTICLE

sulphone group of DDSDP was observed at 1144 cm^{-1}. The band at 2922 cm^{-1} of methylene group of DDMDP and the band at 1244 cm^{-1} corresponding to asymmetric stretch of aromatic ether group of DDEDP was observed. The presence of bands at 1200cm^{-1} of P=O group showed that the DECP had been grafted to the amine. The broad peak around 1428–1603 cm^{-1} represents C=C stretch in benzene rings.

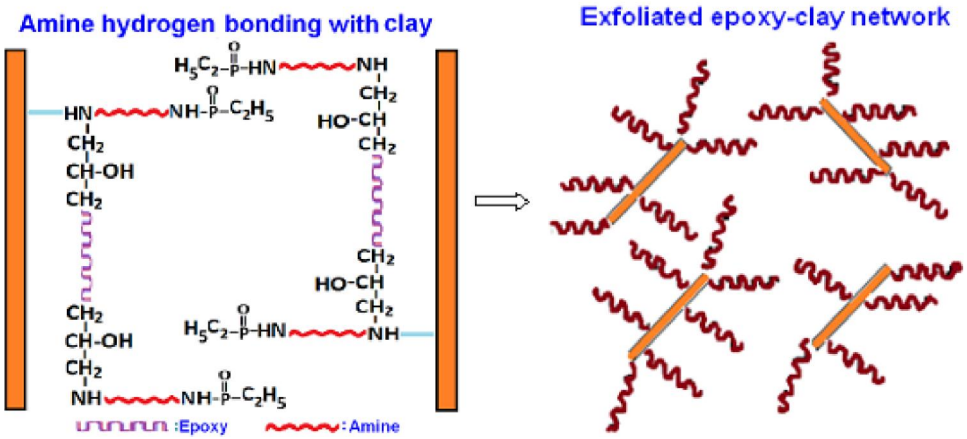

Scheme 2 : Epoxy cured networks with nanoclay with the representation of well intercalated structure formations.

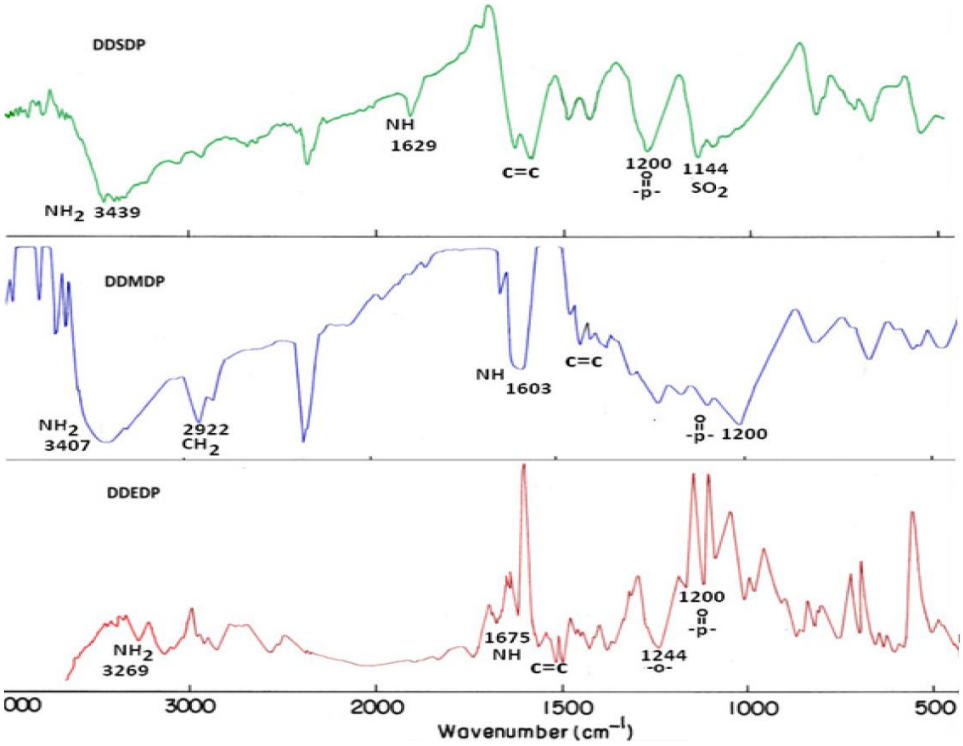

Figure 1 : FT-IR spectra of DDSDP, DDMDP and DDEDP hardeners.

The proton NMR spectra of three PHs were shown in Figure 2. The NH protons and primary amine protons attached to the aromatic ring for DDSDP, DDMDP and DDEDP were observed at 2.9, 2.6 and 2.5, and at 2.4, 2.2 and 2.4ppm respectively. The shift corresponding to methylene protons at 3.7-4.9, 3.7-4.2 and 3.5-3.9, and methyl group protons at 1.0-1.3, 1.2-2.0 and 1.1-2.0, and aromatic protons at 6.5-8.2, 6.5-7.2 and 6.4-7.8 respectively for DDSDP, DDMDP and DDEDP were confirmed the P-hardener structures.

X-ray diffraction (XRD)

Figure 3 shows the XRD pattern of clay modified epoxy systems of DDSDP, DDMDP, and DDEDP.

These epoxy filled with organically modified clay

ORIGINAL ARTICLE

particles did not show the reflection peaks for the d (001) plane due to the stacked clay layer arrangement. This indicated that the clay has moved to a well intercalated region and/or exfoliated region, where the interlayer spacing distance of the clay layers has been increased above 75 nm in which Bragg's law does not obey[14]. Nevertheless, the d (110) plane orientation pertained to the MMT was found around 2=20° whose reflections were not dependant on the distance between the layers. The loss of orientation of the d (001) plane confirms the complete exfoliation of the clay platelets within the epoxy systems.

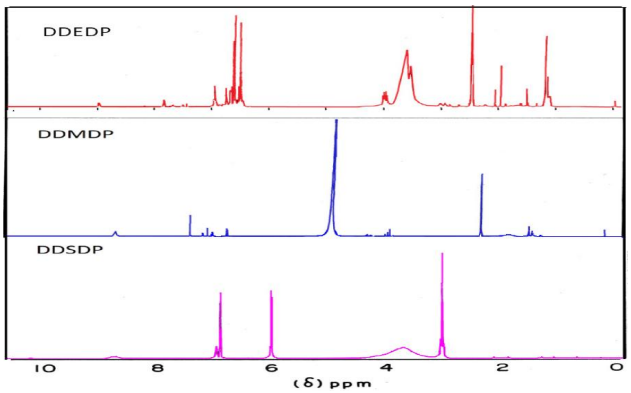

Figure 2 : ^{1}H-NMR spectra of DDSDP, DDMDP and DDEDP.

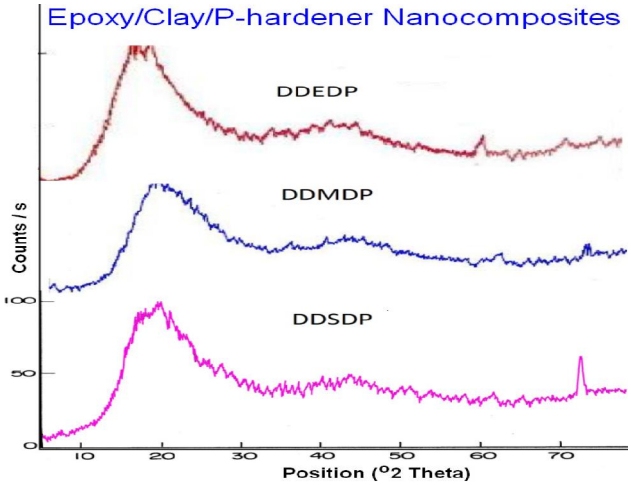

Figure 3 : XRD patterns of CME systems DDSDP, DDMDP and DDEDP hardeners.

TEM analysis of 1.30E nanoclay dispersion

The clay layers have dispersed into the nanosize was studied using transmission electron microscopy (TEM). The 1.30E nanoclay dispersed in acetone was found to be fully delaminated and well dispersed in the acetone solvent. The widths of the exfoliated tactoids were found to be in the range of 10 nm. The TEM picture captured at 100nm magnification was shown in Figure 4.

This TEM morphological observation was in consistent with the XRD analysis which showed the absence of ordered structural patterns.

Thermogravimetric analysis

Figure 5A and 5B represented the TGA curves of UME and CME systems. The UME systems have undergone single stage thermal degradation process and similar IDT behaviour around 319-365°C.

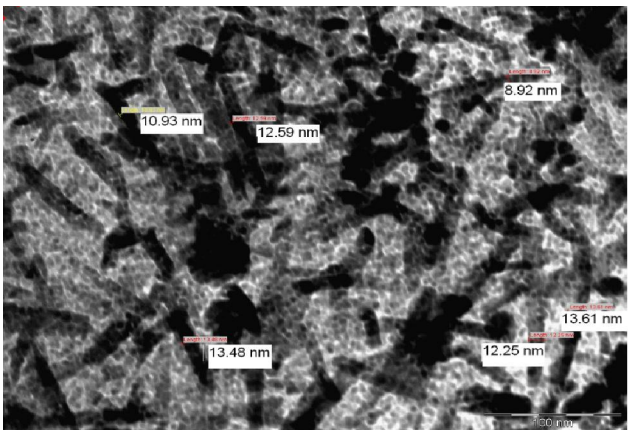

Figure 4 : TEM picture of nanoclay (1.30E, Nanomer) dispersion at 100 nm magnification.

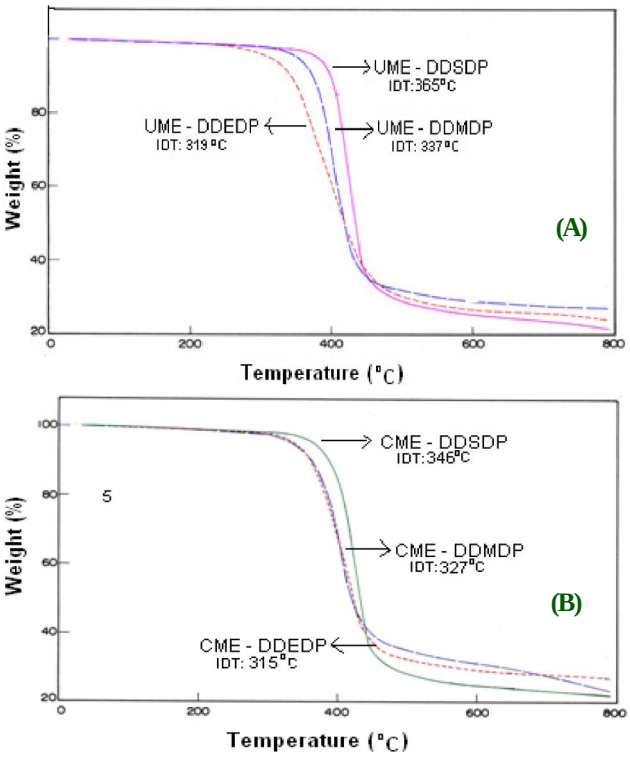

Figure 5 : TGA plots for (A) UME and (B) CME nanocomposites.

ORIGINAL ARTICLE

This was attributed to the homogeneity achieved between DGEBA and PHs. The degradation occurred around 350°C was due to the degradation of chemical bonds of epoxy networks[15]. The relative thermal stability of UME composites and CME nanocomposites was compared by their initial decomposition temperatures (TABLE 2). In the case of UME-DDSDP, the decomposition starts at 365°C. Similarly for UME-DDMDP and UME-DDEDP the decomposition starts at 337°C at 319°C respectively. The presence of sulphone groups in UME-DDSDP seems to give higher initial decomposition temperature over other systems. The lowest IDT value of the UME-DDEDP was due to the presence of the flexible ether groups.

TABLE 2 : TGA property of the UME and CME systems.

Sample	Onset (°C)	Weight loss (%)					MDT (°C)	%Char yield	Oxygen index
		5%	15%	30%	45%	60%			
UME-DDSDP	365	375	398	418	432	440	425	21.3	26.0
UME-DDMDP	337	363	388	403	415	446	355	26.9	26.3
UME-DDEDP	319	325	368	377	399	428	345	23.7	28.3
CME-DDSDP	346	351	385	495	430	442	420	22.0	28.7
CME-DDMDP	327	296	385	403	413	430	355	28.9	27.7
CME-DDEDP	315	330	370	394	411	448	403	25.5	27.9

Note: IDT: Initial decomposition temperature; % Weight loss during heating under non isothermal mode; MDT: Maximum decomposition temperature; % Char: Char residue formed at 800 °C; LOI: Limiting oxygen index obtained through the correlation studies with the char yield quantity formed.

The addition of organoclay to the epoxies shifted the decomposition temperature towards lower temperatures. The initial decomposition temperatures (IDT) observed were 346°C for CME-DDSDP, 327°C for CME-DDMDP and 315°C for CME-DDEDP. The IDT and char yields were high in the case of UME was could be attributed due to the protection of phosphorous molecules present in the hardener that acted as a barrier protecting from volatilizing the epoxy polymer matrix. Similarly the higher char yields obtained in the CME confirmed the presence of inorganic phases like SiO_2, Al_2O_3 and MgO that dominate in the nanocomposites caused such enhanced thermal stability. Further, the presence of, phenyl units in the epoxy and the phosphorous units present in the P-hardener was responsible for the enhanced thermal stability of the nanocomposites. The char yield values of the UME and CME systems were very much high due to the presence of phosphorous molecules.

The flame retardant property was found out from the limiting oxygen index (LOI) value, using the empirical formulae by Krevelen et al[16]. The LOI method helps in determining the relative flammability of polymeric materials. A numerical index, the 'LOI', was representing the minimum concentration of oxygen required to just support burning of a polymer in the air mixture. The higher LOI values represent better flame retardancy.

$$OI \times 100 = 17.5 + 0.4\ CR \quad (1)$$

Where, OI = Oxygen index, and CR = Char residue in weight

The LOI values obtained were increasing with increase in the char yield. The UME-DDMDP and CME-DDMDP showed high OI values. The thermal stability of the systems was further established with the integral procedural temperature (IPDT) studies (TABLE 3). The IPDT[17,18] proposed by Doyle[19] was calculated using Eq. (2)

$$IPDT\ (°C) = A^* K^* (T_f - T_i) + T_i \quad (2)$$

Where, A* represents the area ratio of total experimental curve divided by total TGA thermogram, K* is the coefficient of A*, T_i is the initial experimental temperature, and T_f is the final experimental temperature. The high IPDT values of 552 to 570°C were observed in unmodified systems when compared to 532 to 535°C in the case of modified systems. Thus, the UME systems have exhibited superior thermal stability over the CME systems due to the presence of higher concentration of phosphorous in the crosslinked structures.

TABLE 3 : Determination of IPDT values of UME and CME systems.

Systems	A*	K*	A*K*	IPDT Temp.
UME-DDSDP	0.7064	2.4066	1.7000	548
UME-DDMDP	0.7148	2.5070	1.7920	570
UME-DDEDP	0.7046	2.4496	1.7259	552
CME-DDSDP	0.7067	2.4105	1.7035	532
CME-DDMDP	0.7084	2.4125	1.7090	535
CME-DDEDP	0.7172	2.5362	1.8189	555

ORIGINAL ARTICLE

Kinetics of the thermal degradation[20]

The basic equation used to describe decomposition reactions is

$$\frac{d\alpha}{dt} = k(T)f(\alpha) \quad (3)$$

T rate constant k(T) and f(α) were functions of temperature, and conversion respectively was defined as

$$\alpha = \frac{M_0 - M_t}{M_0 - M_f} \quad (4)$$

Where, M_0: initial sample weight, M_t and M_f were the weight at time t and final sample weight respectively. Usually k is assumed to follow Arrhenius relationship:

$$k = A \exp\left(\frac{-E}{RT}\right) \quad (5)$$

Where A is the pre-exponential factor, R is the universal gas constant, T is the temperature and E is the activation energy. Several models have been proposed to solve the integration of the rate equation. The models selected in this study were Broido[21], Coats-Redfern (C-R)[22] and Horowitz-Metzger's (H-M)[23].

These methods involve TGA curves to find out the kinetics involved in the thermal degradation reactions of the epoxy/P-hardener nanocomposites. These models assume a first order decomposition reaction.

Broido's Method

$$\ln\left[\ln\frac{1}{y}\right] = -\frac{E_a}{R}\frac{1}{T} + \left(\frac{R}{E_a}\frac{A}{\beta}T^2 \max\right)_a \quad (6)$$

Coats-Redfern Method relates the α with T.

$$\ln\left[\frac{-\ln(1-y)}{T^2}\right] = \ln\frac{AR}{\beta E_a}\left(1 - \frac{2RT}{E_a}\right) - \frac{E_a}{RT} \text{ for } n = 1 \quad (7)$$

Horowitz-Metzger method

$$\ln(1-y) = \frac{E_a\left(T - T_p\right)}{R\left(T_p\right)} \text{ for } n = 1 \quad (8)$$

Where, T is the absolute temperature, α is the conversion at temperature T, y is the fraction of initial molecules and not yet decomposed, T_{max} the absolute temperature of maximum reaction rate, β is the rate of heating, A is the frequency factor, DT_{max} is the maximum decomposition temperature and $\theta = T - DT_{max}$, R is the gas constant and E_a is the activation energy. E_a can be determined from the plot of left hand side of each of the equation 6, 7 and 8 versus 1000/T[24,25].

The activation energy data was given in TABLE 4.

TABLE 4 : Determination of activation energies of UME and CME systems.

Sample	Models					
	Kinetic parameters					
	Broido		Horowitz-Metzger		Coats-Redfern	
	E_a	R^2	E_a	R^2	E_a	R^2
UME-DDSDP	281	0.981	295	0.990	278	0.995
UME-DDMDP	152	0.933	192	0.972	163	0.869
UME-DDEDP	171	0.962	171	0.997	192	0.975
CME-DDSDP	235	0.993	216	0.998	226	0.983
CME-DDMDP	123	0.976	130	0.973	160	0.897
CME-DDEDP	166	0.972	171	0.995	175	0.973

Figure 6A-F showed the plots for determining the activation energy of the cured materials degradation. The regression coefficient (R^2) of the each curve and the activation energy (E_a) were obtained from the plot and the slope.

The activation energies of the UME were higher than the CME and they seemed to show similar activation energies as far as the different models are concerned. In the case of UME the increased energy demand for thermal degradation confirmed the enhanced thermal resistance effect of highly crosslinked structure formed in the cured materials. Amongst the UME system, the low activation energy of the DDMDP cured resin was due to the presence of aliphatic methylene bonds. The higher activation energy of DDSDP might be owing to the presence of sulphone atom which has relatively higher thermal-oxidative stability. Further, introducing nanoclay layers have decreased their activation energies of degradation because of the flexibilising effect of the nanoclay which has reflected in lower IDT values.

Dynamic mechanical analysis

The dynamic mechanical analysis measures the storage modulus property (E') that deals in assessing the ability of the materials to store the energy. The storage modulus of UME systems such as UME-DDSDP, UME-DDMDP and UME-DDEDP were found to be 2672, 2708 and 2759 MPa respectively (Figure 7A and B).

While, the storage modulus value (E') observed were 1730 for CME-DDSDP, 2501 for CME-

DDMDP and 4240 Mpa for CME-DDEDP (Figure 8A and B).

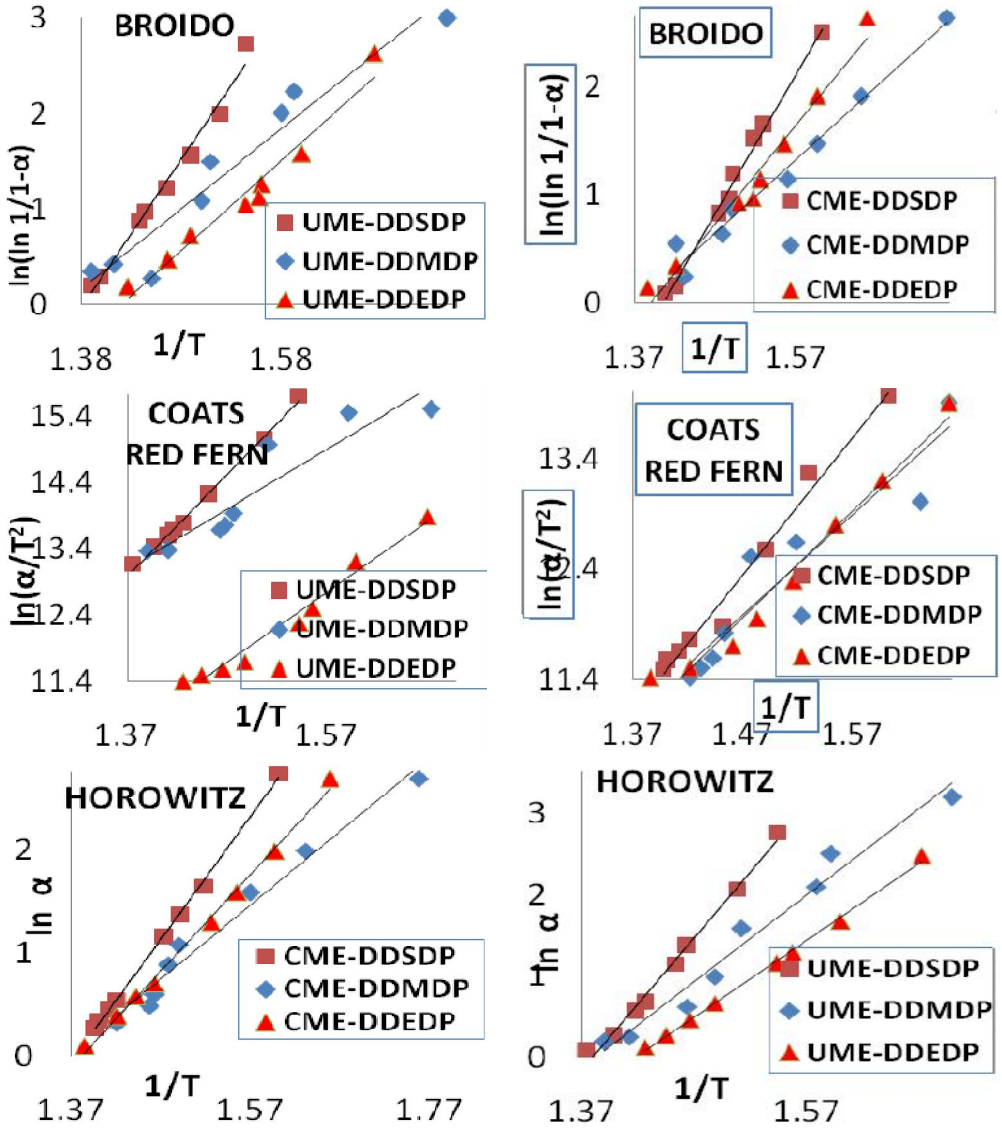

Figure 6 : Activation energy plots of broido, coats-redfern and horowitz metzger models for UME and CME systems.

The storage modulus decreased in the present study compared to the conventional DGEBA/DDS epoxy system[26] was due to the introduction of P-hardener and clay to the resin. This decreased the stiffness due to the flexibility and mobility of chain molecules. Further, the effect of P-hardener or clay on the Tg (relaxation behavior was seen by the decrease in the value of tan δ. The broadening of the curves indicates the restricted segmental motion. The α-transition was related to the Brownian motion of the main chain. The ratio of energy dissipated to energy stored (tan δ), shows a maximum and provides a very sensitive means of analyzing the α-relaxation. It was observed that the Tg values have decreased upon the incorporation of organoclay[27].

The significant decrease in the Tg of the final resin system was due to the intercalated clay structures present in the epoxy systems. The nanoclay layers dispersed in the epoxy resins have hindered the benzene ring mobility because of its high exfoliation that was reflected in high storage modulus and high damping (tan δ) properties. Thus, the polymer relaxation motions will not be constrained because of the presence of clay fillers. Hence, the clay layer acted as a typical toughener. The lowest storage modulus property of the UME-DDMDP and CME-DDMDP systems showed rubber like behaviour due to the methylene links present in the epoxide. The tan δ and Tg of UME systems were very similar to CME systems.

ORIGINAL ARTICLE

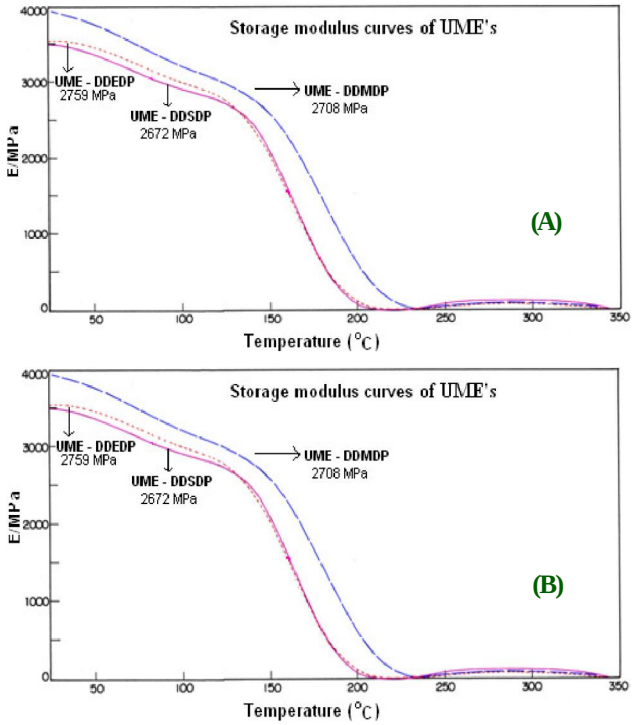

Figure 7(A) : Storage modulus and (B) Tan δ properties of UME systems.

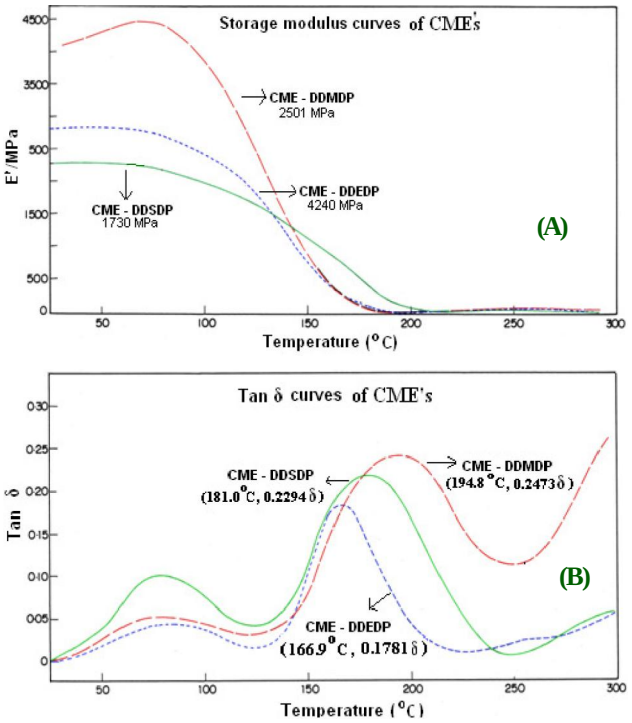

Figure 8(A) : Storage modulus and (B) Tan δ properties of CME systems.

Effect of Crosslink density in UME and CME systems by dynamic mechanical analysis

The crosslink density and the Tg temperatures observed in the systems could be explained by considering the flexibilising effect of the epoxy resins. The effect of addition of P-hardener and clay fillers on the Tg temperature of the cured network structure of the systems were studied. Within both UME and CME systems, it was observed (TABLE 5) that when the crosslinking density was decreased, the glass transition temperature was decreased. The lowest Tg property exhibited by the UME-DDEDP was due to the flexible ether group present in the system. That means the mobility was increased with formation of more open networks. Further, the molecular weight between the crosslinks (Mc) estimated was seemed to be inversely proportional to the Tg and therefore to the crosslink density of the systems (Figure 9).

The rise in the molecular weight between the crosslinking points has increased the spacer length between the crosslinking points. This has helped to form loosed network structures which has resulted into the reduced crosslink density and Tg values. Thus the Tg property which is proportional to the inverse of Mc is shown. Crosslink density could be calculated by using the formula[28].

$$\rho = G'/RT \qquad (9)$$

Where, ρ =Crosslink density expressed in mol/cm^3, G' =Shear storage modulus of the epoxy systems at a temperature well above Tg, R=Universal gas constant (8.314472 J K^{-1} mol^{-1}), T= Absolute temperature (273.15 K) at which the experimental modulus was determined.

TABLE 5 : DMA properties of UME and CME systems: Tg data was obtained through DMA analysis.

Systems	Tg (DMA)	Tan δ_{max} Hz	Storage Modulus E'	Crosslink density ρ	Mc
UME-DDSDP	187.5	0.2372	2672	1.1741	322
UME=DDMDP	201.0	0.2763	2708	2.4211	400
UME-DDEDP	195.5	0.2561	2759	0.7611	290
CME-DDSDP	181.0	0.2294	1730	1.8648	346
CME-DDMDP	194.8	0.2473	2501	1.2132	338
CME-DDEDP	166.9	0.1781	4240	1.8648	386

Note: Tan δmax: The value obtained by the ratio of Storage modulus Vs Loss modulus which expresses the damping ability of the materials.; E': Storage modulus property of the cured materials.; ρ: Crosslinking density of the materials obtained from the formula ρ =G'/RT; Mc: Molecular weight between the crosslinks that helps to find out the kind of crosslinking formed which reflected in Tg, Tan δmax, E' and ρ properties.

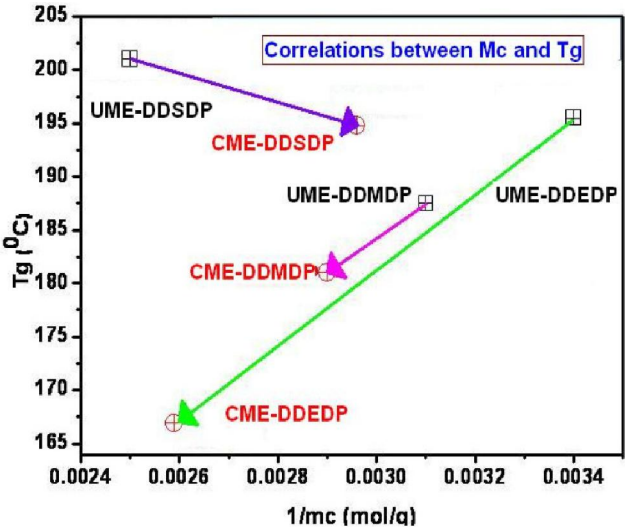

Figure 9 : The correlation study between 1/Mc Vs Tg; Mc: Molecular weight between the crosslinks.

CONCLUSIONS

Three kinds of phosphorus hardeners were successfully prepared and well characterized. The P-hardeners were able to disperse better in the epoxy systems and their amine was expected to link with clay particles and epoxy blends. They were grafted onto epoxy/MMT nanoparticles by using hardeners as compatibilizers and fire retardants in the epoxy formulations. The IDT temperatures of the P-containing UMEs were significantly higher than the CMEs owing to the phospshorous linkages and rigid aromatic substituent that lead to a higher chain stiffness. The epoxy blends containing phosphorus-units in combination with the nanoclay layers led to an increased thermal stability compared to UME systems because of high char yield formed due to the synergistic effect of phosphorous and nanoclays.

REFERENCES

[1] E.P.Giannelis, R.Krishnamoorti, E.Manias; Polymer-silicate nanocomposites model systems for confined polymers and polymer brushes. Advances in Polymer Science, **138**, 107–48 **(1998)**.

[2] T.J.Pinnavaia, G.W.Beall; Polymer-clay nanocomposites, John Wiley and Sons, **(2001)**.

[3] P.Dubois, M.Alexandre; Polymer-layered silicate nanocomposites: preparation, properties and uses of a new class of materials. Materials Science and Engineering R, 1–63 **(2000)**.

[4] A.Okada, A.Usuki; Twenty years of polymer-clay nanocomposites. Macromolecular Materials and Engineering, **291**, 1449–1476 **(2006)**.

[5] P.A.Martinez, V.Cadiz, A.Mantecon, A.Serra; Synthesis, characterization, and thermal behaviour of new epoxy polyesterimides. Angewandte Makromolekulare Chemie, **133**, 97-109 **(1985)**.

[6] A.Mantecon, V.Cadiz, A.Serra, P.A.Martinez; Curing of N,N'-diglycidylimides with polyfunctional compounds. European Polymer Journal, **23**, 481 **(1987)**.

[7] A.Serra, V.Cadiz, P.A.Martinez, A.Mantecon; Preparation and reactivity of new 3,32 , 4,42 - tetracarboxybenzophenone dianhydride glycidyl ester derivatives. Angewandte Makromolekulare Chemie, **140**, 113-125 **(1986)**.

[8] J.A.Mikroyannidis, D.A.Kourtides; Advances in Chemistry Series, **208**, 351 **(1984)**.

[9] J.A.Mikroyannidis, D.A.Kourtides; Curing of epoxy resins with 1-[di(2-chloroethoxyphosphinyl) methyl]-2,4-and -2,6-diaminobenzene. Journal of Applied Polymer Science, **29**, 197 **(1984)**.

[10] M.Lewin, S.M.Atlas, E.H.Pearce; Flame retardant polymeric materials, Plenum, New York, **1**, 22 **(1975)**.

[11] W.K.Chin, M.D.Hsau, W.C.Tsai; Synthesis, structure and thermal properties of epoxy- imide resin cured by phosphorylated diamine. Journal of Polymer Science Part A: Polymer Chemistry, **33**, 373 **(1995)**.

[12] Li Chen, Yu-Zhong Wang; A review on flame retardant technology in china. Part I development of flame retardants. Polymers for Advanced Technologies, **21(1)**, 1–26 **(2009)**.

[13] M.Suguna Lakshmi, H.H.Omar Ashwaq, B.S.R.Reddy; Synthesis and characterization of novel phosphrous-coupling agent for use as compatibilizer, flame retardant, hardener and adhesion promoter in making polymer networks. Polymer - Plastics Technology and Engineering Journal, **50**, 266–275 **(2011)**.

[14] Asma Yasmin, J.L.Abot, I.Daniel; Processing of clay/epoxy nanocomposites by shear mixing. Scripta Materiala Journal, **49**, 81–6 **(2003)**.

[15] G.Camino, G.Tartaglione, A.Frache; Thermal and combustion behaviour of layered silicate-epoxy nanocomposites. Polymer Degradation and Stabilility Journal, **90**, 354–62 **(2005)**.

[16] D.W.Van Krevelen; Some basic aspects of flame

ORIGINAL ARTICLE

resistance of polymeric materials. Polymer, **16**, 615–620 **(1975)**.

[17] S.J.Park, H.C.Kim, H.I.Lee, D.H.Suh; Thermal stability of imidized epoxy blends initiated by N-benzylpyrazinium hexafluoroantimonate salt. Macromolecules, **34**, 7573 **(2001)**.

[18] C.L.Chiang, S.W.Hsu; Synthesis, characterization and thermal properties of novel epoxy-expandable graphite composites. Polymer International Journal, **59(1)**, 119–126 **(2010)**.

[19] C.D.Doyle; Termogravimetric analysis: In encyclopedia of polymer science and engineering, Wiley Interscience Publishers, New York, **14**, 1–41 **(1985)**.

[20] A.Al-Mulla, H.I.Shaban; Thermal degradation of poly(trimethylene terephthalate) and acrylonitrile butadiene styrene blends: kinetic analysis of thermogravimetric data. International Journal of Polymeric Materials, **57(3)**, 275–87 **(2008)**.

[21] A.Broido; A simple, sensitive graphical method of treating thermogravimetric analysis data. Journal of Polymer Science Part A: Polymer Chemistry, **7**, 1761–73 **(1969)**.

[22] A.W.Coats, J.P.Redfern; Kinetic parameters from thermodynamic data. Nature, **201**, 68–69 **(1964)**.

[23] H.H.Horowitz, G.Metzger; New analysis of thermogravimetric traces. Analytical Chemistry Journal, **35**, 1464 **(1963)**.

[24] M.A.Ashok, B.N.Achar; Thermal decomposition kinetics and solidstate, temperature dependent, electrical conductivity of charge-transfer complex of phenothiazine with chloranil and picric acid. India Academy of Sciences (Bulletin of Material Science), **31(1)**, 29–35 **(2008)**.

[25] K.S.Muralidhara, S.Sreenivasan; Thermal degradation and burning behaviour of cotton, polyester and polyester/cotton blended upholastery fabrics. Journal of World Applied Sciences Journal, **9(11)**, 1272–1279 **(2010)**.

[26] M.Srividhya, M.Suguna Lakshmi, B.S.R.Reddy; Chemistry of siloxane amide as a new curing agent for epoxy resin: Materials characterization and properties. Journal of Macromolecular Chemistry and Physics, **206(24)**, 2501–2511 **(2005)**.

[27] J.Massam, T.J.Pinnavaia; Clay nanolayer reinforcement of a glassy epoxy polymer. Materials Research Society Symposium Proceedings, **520**, 223–32 **(1998)**.

[28] L.W.Hill; Dynamic mechanical and tensile properties. In: J.V.Koleske (Ed); Pain and coating testing manual, ASTM International, Philadelphia, **46**, 534–46 **(1995)**.